Bioinformatics, 2020, 1–7
doi: 10.1093/bioinformatics/btaa969
Advance Access Publication Date: 16 November 2020
Original Paper

Systems biology

Agent-based modeling reveals benefits of heterogeneous and stochastic cell populations during cGAS-mediated IFNβ production

Robert W. Gregg [1], Fathima Shabnam[1] and Jason E. Shoemaker[1,2,3,*]

[1]Department of Chemical and Petroleum Engineering, 15260, [2]McGowan Institute for Regenerative Medicine, 15219 and [3]Department of Computational and Systems Biology, University of Pittsburgh, Pittsburgh, PA 15260, USA

*To whom correspondence should be addressed.

Associate Editor: Pier Luigi Martelli

Received on May 7, 2020; revised on October 13, 2020; editorial decision on November 3, 2020; accepted on November 4, 2020

Abstract

Motivation: The cGAS pathway is a component of the innate immune system responsible for the detection of pathogenic DNA and upregulation of interferon beta (IFNβ). Experimental evidence shows that IFNβ signaling occurs in highly heterogeneous cells and is stochastic in nature; however, the benefits of these attributes remain unclear. To investigate how stochasticity and heterogeneity affect IFNβ production, an agent-based model is developed to simulate both DNA transfection and viral infection.

Results: We show that heterogeneity can enhance IFNβ responses during infection. Furthermore, by varying the degree of IFNβ stochasticity, we find that only a percentage of cells (20–30%) need to respond during infection. Going beyond this range provides no additional protection against cell death or reduction of viral load. Overall, these simulations suggest that heterogeneity and stochasticity are important for moderating immune potency while minimizing cell death during infection.

Availability and implementation: Model repository is available at: https://github.com/ImmuSystems-Lab/AgentBasedModel-cGASPathway.

Contact: jason.shoemaker@pitt.edu

Supplementary information: Supplementary data are available at *Bioinformatics* online.

1 Introduction

IFNβ expression—a critical component of the innate immune response—has been identified as an inherently stochastic process regulated by interacting, highly heterogeneous cells (Leviyang *et al.*, 2018; Rand et al., 2012; Zhao et al., 2012); however, the consequences stochastic processes and heterogeneous populations bring to innate immune signaling remains an open topic of study. Here, stochasticity is defined as differential responses observed from individual cells given identical stimuli, and heterogeneity is defined as differences between intracellular molecular concentrations across a cell population (which leads to variations in cellular response).

Multiple intrinsic and extrinsic mechanisms have been proposed to explain stochasticity and heterogeneity (Rand *et al.*, 2012; Swain et al., 2002; Zhao *et al.*, 2012). Low intracellular molecular concentrations are a common intrinsic source of stochasticity because they result in probabilistic responses within the cell (e.g. transcriptional busting) (Elowitz, 2002; Raj et al., 2008; Satija et al., 2014). This source of noise can amplify and propagate down signaling pathways affecting gene expression and cellular behavior (Bar-Even *et al.*, 2006). In contrast, extrinsic sources that can cause stochasticity and heterogeneity are differences in the immune stimulus as well as cellular division (Rand *et al.*, 2012; Schulte et al., 2014). Together, these layers of noise and variability coalesce to explain the complex dynamics observed in IFNβ signaling.

The benefits stochasticity and heterogeneity bring to innate immune signaling remain unclear. Some evidence suggests that cells optimize the innate immune response to simultaneously minimize pathogenic loads and maximize cell survival (Zhao *et al.*, 2012). This is plausible as overexpressing innate immune cytokines can cause unnecessary damage to the host (Hwang *et al.*, 2013), leading to cytokine storms and chronic inflammation (Prinz et al., 2012). More recent evidence suggests that stochasticity allows a cell population to subdivide, where some cells produce substantial immune responses that risk apoptosis, while others are preserved to maintain tissue viability (Drayman et al., 2019; Ivashkiv et al., 2014; Raj *et al.*, 2008).

In contrast, hypotheses elucidating the advantages of cellular heterogeneity are less developed. One potential explanation is bet-hedging (Goldman et al., 2019) where less-fit individuals are maintained as a precaution to drastic changes in the environment. Others suggest that heterogeneity acts as an additional layer of non-genetic

variability (Brock *et al.*, 2009; Kim et al., 2018) which can impede pathogenic threats susceptible to noise (Heldt *et al.*, 2015). To better understand stochasticity and heterogeneity in the context of IFNβ immune signaling, computational modeling is employed to simulate cell populations with and without these attributes.

Here, we implement an Agent-Based Model (ABM) of the cGAS pathway, a critical component of the innate immune system responsible for the detection of foreign DNA and expression of IFNβ (Sun et al., 2013). This method was chosen because it extends previous modeling efforts (Gregg *et al.*, 2018) to incorporate stochasticity/heterogeneity and has shown success in similar cell signal modeling (Id *et al.*, 2020; Rikard et al., 2019; Roy et al., 2019; Warsinske et al., 2016). In this context, success implies correctly emulating biological outcomes and predicting behavior using a robust and stable model. Utilizing computational models that incorporate these attributes has allowed researchers to simulate outcomes that are difficult to resolve with experimental techniques alone, such as predicting therapies that impede heterogeneous tumors (Roy *et al.*, 2019) and predicting bacterial dissemination in heterogeneous granuloma formation (Id *et al.*, 2020).

Due to the expansive roles cGAS plays in disease detection [e.g. cancer (Ng et al., 2018), inflammation (Gray et al., 2015), acute kidney injury (Maekawa et al., 2019), HSV (Su et al., 2017), HIV (Gao *et al.*, 2013), MTB (Collins *et al.*, 2015)], it is imperative to further explore this signaling pathway to improve new drug therapies (Lama et al., 2019), cancer immunotherapies (Li et al., 2019; Su et al., 2019) and vaccine adjuvants (Wang et al., 2016). To accomplish this, the ABM is used to identify the immunologic advantages a cell population may have when individual cells are heterogeneous and subject to stochastic intracellular IFNβ signaling. We hypothesize that heterogeneity and stochasticity benefit an immune signaling cell population by reducing the required number of IFNβ producing cells while still successfully clearing the pathogenic threat.

2 Materials and methods

2.1 Defining epithelial cell (agent) responses to infection

The ABM is constructed on a 200 by 200 grid where each agent represents an epithelial cell (40 000 cells total, see Fig. 1). The agents—as they are epithelial cells—remain stationary, while paracrine signaling dynamics allow neighboring agents to transmit information about their current state and influence the population. Grid sections are sized such that the edge is roughly equivalent to the diameter of a human epithelial cell (32 μm), which provides the proper scale for diffusion (Cohen *et al.*, 1967; Milo *et al.*, 2015).

ABMs are flexible frameworks that can use rules, algebraic equations or ODEs to define how agents respond to their environment. Here, each agent possesses an ODE model and probabilistic rules that dictate how they respond to changing local DNA and IFNβ concentrations as well as the number of virions in neighboring agents. The ODE model (Gregg *et al.*, 2018) describes how signaling mechanisms within agents respond to current local concentrations of IFNβ and DNA. The differential equations remained largely unchanged, except for the addition of the diffusion term for IFNβ to support integrating the ODE system into the ABM:

$$\frac{\partial[\text{IFN}\beta]}{\partial t} = \frac{k_{\text{cat7}}[\text{IFN}\beta\text{mRNA}]}{K_{m7} + [\text{IFN}\beta\text{mRNA}]} - \tau_7[\text{IFN}\beta] + D\nabla^2[\text{IFN}\beta]. \quad (1)$$

Parameters used to simulate each agent are taken from the best (i.e. lowest error) MCMC iteration of the original work. Two independent sources were found for the diffusion coefficient of IFNβ [95 μm^2/s (Kreuz *et al.*, 1965) and 100 μm^2/s (Coppey *et al.*, 2007)] so an average of the two are used in the simulation.

The ABM also uses probabilistic rules that facilitate changes in cell state and propagation of the infection. The first rule states the probability that a healthy cell transitions into an infected cell depends on the adjacent cell's viral concentrations (i.e. Moore's neighbors). Each cell is assigned a viral load threshold value randomly sampled from a normal distribution with a mean of 800 virions and standard deviation of 200 virions. When an infected cell's viral concentration exceeds its given threshold, it attempts to infect each healthy neighboring cell through a Bernoulli trial with the probability of success defaulted to 0.5. Modifying this parameter effects how quickly the infection spreads throughout the population, with low values effectively halting viral spread. To track viral load over time, an additional ODE state 'Virus' is added to the ABM and the DNA state is modified to incorporate replication,

$$\frac{\text{d}[\text{Virus}]}{\text{d}t} = k_{14f}[\text{DNA}] - \tau_{14}[\text{Virus}] \quad (2a)$$

$$\frac{\text{d}[\text{DNA}]}{\text{d}t} = -k_{1f}[\text{cGAS}][\text{DNA}] + k_{1r}[\text{cGAS}_{\text{complex}}] - \times \frac{k_{\text{cat2}}[\text{TREX1}][\text{DNA}]}{K_{m2} + [\text{DNA}]} + \frac{[\text{DNA}](K_{\max} - [\text{DNA}])}{K_{\max}}. \quad (2b)$$

The second probabilistic rule determines the initial concentration of viral DNA after a cell becomes infected. This is simulated in the model as a discontinuous jump in DNA concentration subject to a uniform distribution on the interval [0, $K_{\max}$]. The modified DNA state can now vary with cGAS binding, TREX1 degradation or replication specified by the carrying capacity ($K_{\max} = 0.55$ nM).

The third and last probabilistic rule depends on the randomly assigned infection length time, also sampled from a normal distribution with a mean 8 h and standard deviation of 1 h. When an infected cell surpasses the allotted time to be infected, a callback event is triggered that sets all parameters associated with transcription and translation to a value of zero, and the cell is assigned to a dead state. Proteins, mRNA and other molecules quickly degrade because the cellular agent has no means to sustain their concentrations.

2.2 Agent-based model simulation

The ABM is simulated in Julia, which offers several advanced packages for rapid simulation. At each timestep, the probabilistic rules are checked and each cell state is updated accordingly. After the update, the DifferentialEquations.jl package (Rackauckas *et al.*, 2017) is used to progress the intracellular concentrations forward in time. The Laplacian modeling the diffusion process is discretized using a second order central differencing scheme with no flux boundary conditions. This discretization, combined with intracellular ODEs, results in an ABM with 520 000 ODEs (13 per agent) and 120 000 probabilistic rules (3 per agent). A model of this scale requires a well-optimized solver that is efficient in computing time and memory, as well as being numerically stable (Perkel, 2019). We used an implicit ODE solver [backward differentiation formula, BDF (Hindmarsh *et al.*, 2005)], which eliminated numerical instability but required solving a system of linear equations at each time step. Instead of solving the linear system directly, we used a generalized minimal residual method (GMRES) to accelerate the BDF solver (Saad *et al.*, 1986).

Two initial conditions are implemented in the model depending on whether an ISD transfection or viral infection was simulated. When considering ISD, agents/cells are assigned specific concentrations of viral DNA at time zero. The viral infection initial condition instead assumes each cell within the population has some probability of being initially infected according to a Poisson distribution,

$$P(n) = \frac{\text{MOI}^n \cdot e^{-\text{MOI}}}{n!}. \quad (3)$$

Here, n refers to the number of times a cell is infected, and MOI is the multiplicity of infection. The fraction of cells initially infected (i.e. primary cells) is varied by changing MOI. A low dose simulated infection, for example, would have an MOI of 10^{-3}, which corresponds to an average of 40 cells being initially infected at least once. The remaining, healthy cells with no initial DNA concentration are categorized as secondary cells.

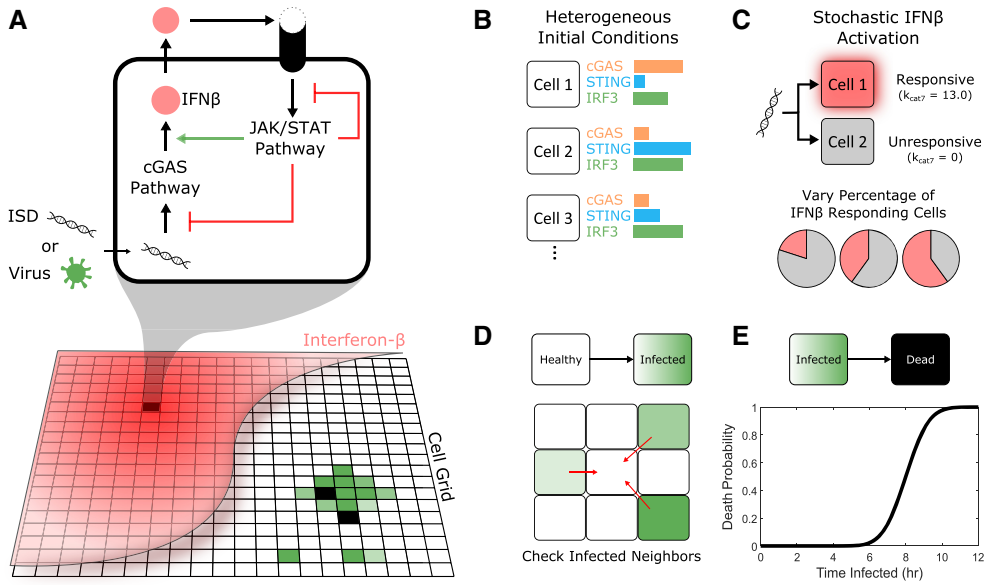

Fig. 1. Overview of the agent-based model. (**A**) The model consists of a bottom grid of cells (agents) and a top layer (agent environment) portraying IFNβ diffusing across the cells. The grid layer is colored green according to the internal DNA concentration (viral or ISD). Healthy cells are colored white and dead cells are colored black. Each cell possesses an ODE model of the cGAS and JAK/STAT signaling pathways which allows for the detection of cytosolic DNA, production of IFNβ and upregulation of feedback mechanisms. (**B**) Heterogeneity is simulated by altering non-zero initial conditions. Initial conditions are sampled from a normal distribution and assigned to each cell at the beginning of the simulation. (**C**) Cells stochastically respond to DNA stimulus by either producing IFNβ (responsive) or by producing no IFNβ (unresponsive). The percentage of responsive cells is varied across simulations. (**D**) Healthy cells transition into an infected state subject to the viral concentrations of neighboring cells (Moore neighborhood). As the concentration of virus increases within an infected cell, the probability of infecting a neighboring cell also increases. (**E**) Infected cells then transition into dead cells over time with increasing probability

2.3 Cellular heterogeneity and stochasticity

Experimental observations show that cells possess diverse intracellular molecular concentrations (heterogeneity) and respond in a binary manner (stochasticity). To model these observations, we varied initial conditions and randomly modified ODE parameters associated with IFNβ production. Initial conditions are varied by sampling from a truncated normal distribution (bounds 0 to infinity) with a mean specified by the original initial condition and a set variance. By surveying different variances, we can determine how sensitive the interferon response is to heterogeneity in cellular composition. The default variance was set to 0.5 nM^2. To simulate the outcome of stochastic IFNβ signaling, cells are randomly assigned different k_{cat7} values (Equation 1). This parameter is responsible for IFNβ mRNA translation and is treated as a Bernoulli distributed random variable with the probability of failure equal to the desired percentage of interferon producing cells. The default percentage was set to 20%.

2.4 Statistical analysis

Comparison between group means was performed using a two-sample *t*-test in R version 3.6.3. *P*-values were adjusted using a Bonferroni correction to account for multiple comparisons. An adjusted *P*-value <0.01 was considered significant.

3 Results

3.1 Stochasticity and heterogeneity modulate IFNβ and conserve cell survival

With the development of the ABM (Fig. 1), we evaluated the model's ability to replicate different population-level (i.e. bulk-level) experimental results and analyzed the effects of stochasticity and heterogeneity on cGAS signaling, virus growth and cell death. To compare across the various model simulations, we monitored IFNβ signaling at the cell population level.

Figure 2 illustrates the IFNβ distribution and cell (agent) state (healthy, infected, dead) across the cell population 10 h after an initial ISD transfection (Fig. 2A and D) or DNA virus infection (Fig. 2B, C, E, F). (See Supplementary Video S1 for full-time course). Simulations were performed under homogeneous/deterministic or heterogeneous/stochastic conditions to compare outcomes (see Supplementary Fig. S1 for other combinations). During ISD transfection (Fig. 2A and D), a dashed-lined boundary divides the population into primary cells, which directly receive an ISD transfection and secondary cells, which receive no direct DNA stimulus and only respond to paracrine IFNβ signaling. Transfection simulations with homogeneous/deterministic cell populations (Fig. 2A) exhibited higher overall IFNβ production and more secondary cell activation than observed in a heterogeneous/stochastic cell population (Fig. 2D).

Viral infection simulations exhibited different IFNβ profiles (Fig. 2B and E), but the number of cells dead at hour 10 is comparable in both viral infection simulations (Fig. 2C and F), at 5.3% and 4.5%, respectively. These results suggest that stochasticity and heterogeneity together significantly influence the amount of IFNβ produced (in this case reducing IFNβ); however, this influence does not extend to cell survival, as it remains unchanged. Stochasticity and heterogeneity appear to benefit the cell population by diminishing the response needed to overcome the same threat. To further develop this hypothesis, the following sections will investigate how stochasticity and heterogeneity affect intracellular signaling and determine how each impacts the immune response.

3.2 Dynamics of intracellular molecules are consistent with experimental evidence

We tested the ABM to see if it could replicate bulk intracellular signaling from cells challenged with ISD and virus (Fig. 3 and Supplementary Fig. S2). During ISD transfection (Fig. 3A–H) we observe a strong IFNβ response in primary cells to the DNA stimulus, followed by activation feedback mechanisms like IRF7 and TREX1. The dynamic responses of the primary cells result from our previous work fitting an ODE model to 10 experimental datasets [see Supplementary Fig. S2 (Cox *et al.*, 2017; Guo *et al.*, 2017; Jønsson *et al.*, 2017; Posselt *et al.*, 2011; Qing *et al.*, 2004; Sun *et al.*, 2013; Wang et al., 2017)] and we show that the ABM reproduces those

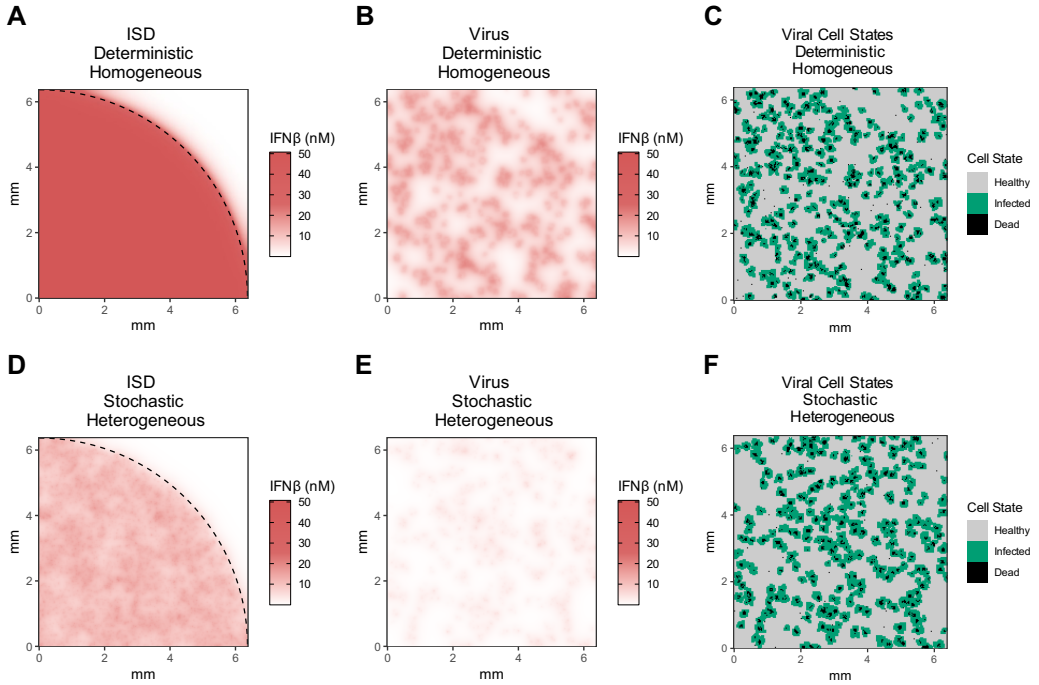

Fig. 2. Simulating IFNβ dynamics across different cell (agent) populations. The distribution of IFNβ 10 h after the addition of cytosolic DNA (viral or ISD). Cell populations were either modeled as deterministic and homogeneous (**A–C**) or stochastic and heterogeneous (**D–F**). For other combinations see Supplementary Figure S1. Panels (A) and (D) show cell populations transfected with immunostimulatory DNA (ISD). The quarter circular region (dotted black line) divides the cells into two populations. Cells within the boundary were transfected with ISD and referred to as primary cells. Cells outside this region were not transfected and referred to as secondary cells. In panels (B) and (D), a virus infection is simulated by assigning non-zero initial conditions of DNA according to a Poisson distribution with MOI = 0.01 (Equation 2). Panels (C) and (F) show the same viral simulation but identify cell states (healthy, infected or dead)

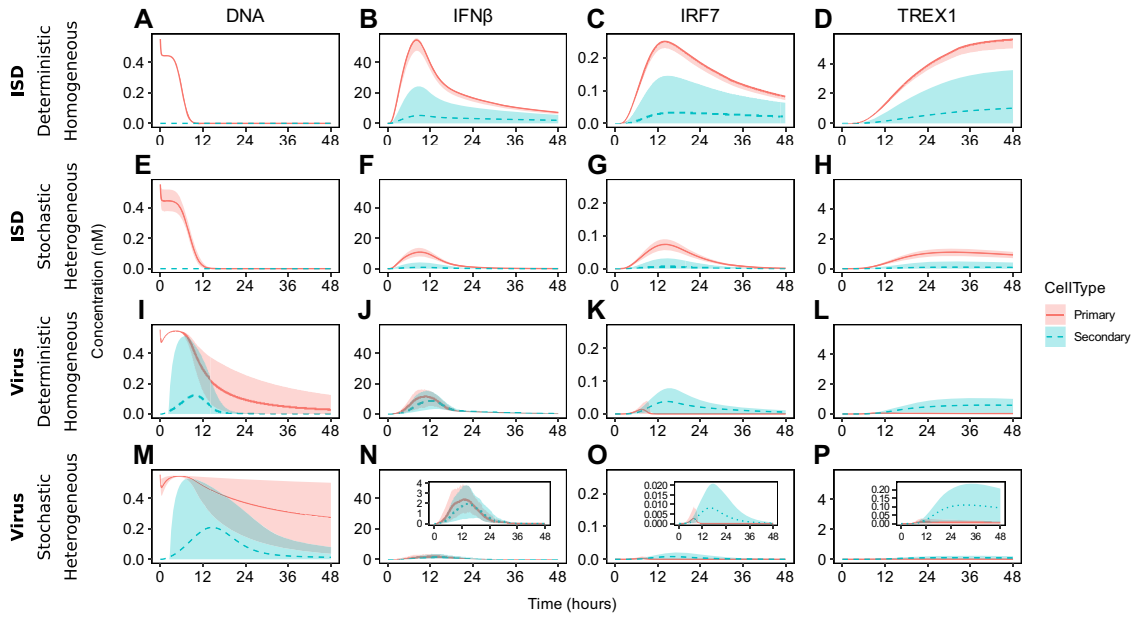

Fig. 3. Simulating intracellular dynamics across different cell populations. The intracellular signaling dynamics in response to ISD transfection (**A–H**) and viral infection (**I–P**) under deterministic/homogeneous (A–D, I–L) or stochastic/heterogeneous (E–H, M–P) conditions. Average intracellular concentrations are plotted as a function of time and are separated into cells that are initially transfected/infected (primary) and those that are not (secondary cells). The bold line represents the mean trajectory within the population of 40 000 cells (agents) with error bands showing the 5th and 95th percentiles. Panels N–P have inset figures to show more detailed dynamics on a smaller scale

findings when most cells are infected. Note that secondary cells respond to IFNβ paracrine signaling to a lower degree and do not follow experimental results because the available experiments were performed with high MOIs, meaning almost all cells were primary cells.

Viral infection simulations (Fig. 3I–P) show an enhanced response from secondary cells, particularly from feedback mechanisms like IRF7 (Fig. 3K and O) and TREX1 (Fig. 3L and P). The variance in these responses is also increased—especially in stochastic/heterogeneous cell populations. This is caused by some secondary cells not

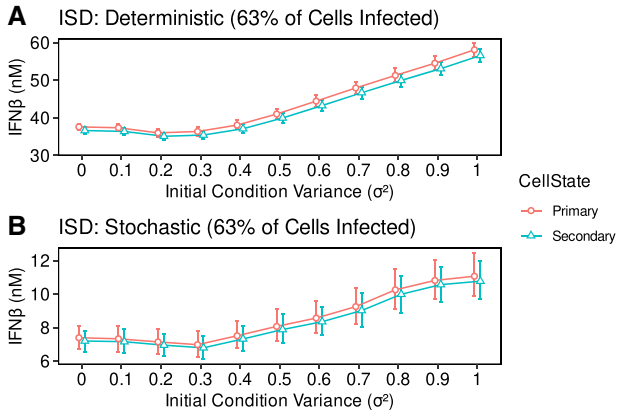

Fig. 4. Effect of heterogeneity on population IFNβ levels. Initial non-zero protein concentrations were sampled from increasingly wider (more variable) normal distributions, as shown on the horizontal axis. With this new initialization, the agents were simulated with an ISD infection starting with 63% primary cells. The resulting distribution of peak IFNβ concentrations were taken and partitioned into either primary or secondary cells. Points represent the median peak IFNβ concentration (25 200 primary cells and 14 800 secondary cells) with error bars showing the interquartile range. The cell population was simulated with (**A**) deterministic IFNβ producing cells and (**B**) stochastic IFNβ producing cells

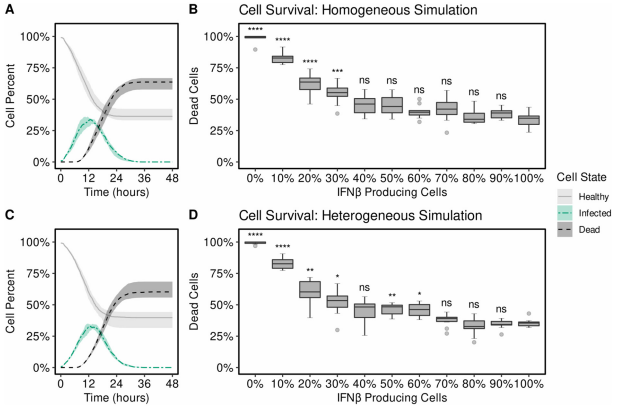

Fig. 5. Stochasticity optimizes cell survival. Stochastic interferon expression of viral infection in homogeneous (**A–B**) and heterogeneous (**C–D**) cell populations. (A) Cell (agent) states were tracked over time in ten simulations with 20% of cells producing IFNβ to obtain median trajectories with the shaded region showing the interquartile range. (B) Each boxplot summarizes the percentage dead cells for ten viral infection simulations (at $t = 48$ h). The percentage of cells producing IFNβ was varied from 0% (no cells producing IFNβ) to 100% (all cells producing an IFNβ). (C) The process was repeated with a heterogeneous cell population, showing cells states where 20% of cells could produce IFNβ. (D) The percentage of IFNβ producing cells was again varied and the percentage dead cell was recorded. Asterisks represent Bonferroni adjusted significant *P*-values from a two-sample *t*-test when compared against the 100% IFNβ producing population (****$P < 0.00001$; ***$P < 0.0001$; **$P < 0.001$; *$P < 0.01$; ns, not significant)

responding to infection while others are responding more than even primary cells (see Supplementary Fig. S3 for secondary cell response distribution). Overall, this suggests that primary cells are more important to ISD transfection and that secondary cells play a more central role in regulating viral infections.

To further support the ABM, we examined the impact heterogeneity and stochasticity had on knockdown simulations. This was compared with simulations of the ODE model under the same knockout conditions. In principle, emergent behavior from the ABM should match bulk cell predictions from the ODE model, which is observed for both TREX1 and IRF7 knockdown (see Supplementary Fig. S4). Note that variability in the deterministic/homogeneous simulations arose from differences in local IFNβ concentrations across the cell population.

3.3 Cellular heterogeneity increases interferon production

The concentrations of mRNA and signaling proteins at the initial time of infection vary across the cell population and are suspected to impact immune signaling dynamics (Wimmers et al., 2018). Figure 4 shows the distribution of peak IFNβ concentrations across the cell population that result when simulating an ISD transfection in a deterministic/heterogeneous (Fig. 4A) or a stochastic/heterogeneous cell population (Fig. 4B). Cells were divided into primary and secondary cells (see Fig. 3) to distinguish production in transfected cells and paracrine-induced IFNβ production, respectively. As increasing Gaussian noise is added to the initial conditions, we observe a small decrease in peak IFNβ produced (Fig. 4A and B, σ^2=0 to σ^2=0.3) followed by a large increase in IFNβ produced (Fig. 4A and B, σ^2=0.4 to σ^2=1.0) as cellular heterogeneity increases. Secondary cells produce less interferon than their primary counterparts across all levels of variability and model types, which indicates that DNA is a more potent IFNβ stimulus compared to interferon alone. These simulations suggest that increasing cellular heterogeneity leads to higher levels of IFNβ production, but moderate levels of heterogeneity can lower IFNβ production independently of stochasticity.

3.4 There is an optimal level of intrinsic stochasticity

To assess how stochasticity and cell heterogeneity impact immune success, we tracked the number of healthy, infected and dead cells during virus infection (Fig. 5). Figure 5A and C show the median trajectories and the interquartile ranges of the cell states in a homogeneous/stochastic or heterogeneous/stochastic cell population, respectively. In both cell populations, the percentage of IFNβ producing capable cells is left at the default value of 20%. Both the homogeneous and heterogeneous cell populations have the largest percentage of cells infected within the first 12 h of simulation and transition to dead based on the randomly assigned duration of infection (see Methods).

An optimal host immune response would minimize both cell death and IFNβ needed to remove cytosolic DNA. With these criteria, we evaluated the cell population's response by changing the number of IFNβ producing cells. This was accomplished by randomly assigning the k_{cat7} parameter (Equation 1) a value of zero based on the desired percentage of IFNβ producing cells (e.g. no IFNβ producing cells would imply that all k_{cat7} parameters were set to zero). Figure 5B shows how viral infection simulations were affected by the percentage of IFNβ producing cells in a homogeneous population. When fewer cells respond to the virus, more cells die; however, there is a wide range (40–100%) where the interferon response varies but cell survival is not significantly affected. A range of 20–30% appears to be the optimal percentage of IFNβ producing cells because it both minimizes the number of cells lost to the infection and IFNβ needed to bolster an effective immune response. Figure 5D repeats these simulations, but with a heterogeneous cell population. There were no apparent differences found between the two cell populations, indicating stochasticity was primarily responsible for the observed trends in cell survival.

4 Discussion

Using a multiscale ABM that reproduces cell culture IFNβ dynamics, we performed *in silico* experiments to determine how cellular heterogeneity and stochasticity impact overall IFNβ production and cell death experienced during the infection. Figure 4 exemplifies how cell heterogeneity can modify intracellular immunity. Low heterogeneity (i.e. small variations in cellular composition) allows a cell population to attain similar IFNβ concentrations without having every cell fully respond with equal magnitude to the infection. Without impacting the overall immune response, heterogeneity allows some cells to express low levels of IFNβ because they are compensated by higher expression from neighboring cells through

paracrine signaling. Highly heterogeneous cell populations magnify this behavior by having only a few cells produce large amounts of IFNβ that can compensate for the rest of the population. A heterogeneous cell population benefits from neighboring cells relying on each other for IFNβ signaling, but taken to an extreme, may lead to an excessive response.

Stochasticity, in comparison, plays an important role in maintaining cell survival. Experimental evidence shows that IFNβ response is stochastic and results in approximately 20% of cells responding to infection (Zhao *et al.*, 2012). The ABM simulates this behavior by varying the number of IFNβ producing cells/agents (Fig. 5). We observed that having 20–30% interferon producing cells resulted in an optimal balance between limiting cell death and producing high concentrations of IFNβ. The modeled ideal percentage of responding cells differs slightly from the number reported by Zhao *et. al.*, but other experimental studies suggest that this ideal response is virus specific (Patil *et al.*). The ABM provided here can easily be modified to fit any viral specific IFNβ response and, more importantly, provides a possible explanation for these experimental observations.

The ABM presented enables consideration of how spatial variation, stochastic signaling within agents and agent/cell heterogeneity impact infection outcomes. However, trade-offs were made when developing this ABM; most notably was the number and complexity of the agents. The model assumes cells are static entities on a uniform grid, which is suitable when modeling epithelial cells, but limits modeling other cell types that require agents to possess attributes like shape, movement and cellular division. The provided code can be modified to consider these attributes and other software, e.g. Compucell3D and Morpheus, can facilitate such studies. Another limitation is how stochasticity is implemented. Stochastic differential equations could be utilized as they would allow for simulating stochasticity due to low molecular copy numbers. However, such an approach would be prohibitively slow, reducing our capacity to simulate cGAS signaling behaviors over a large cell population. Lastly, a consequence of translating the ODE system into each agent was a reduced interferon response (compare Fig. 2A and B). This reduction is caused by the diffusion of IFNβ away from infected cells to neighboring healthy cells, driven by a steep concentration gradient. This dissipative effect is only observed in viral infection simulations because the initial condition for ISD transfection places all primary cells beside one another. This could be addressed with model rescaling (the data informing the model is relative), should non-relative measurements become available.

Overall, this paper develops a straightforward method to translate a signaling pathway model—which are commonly described with ODEs—into an ABM that considers spatial variation, cell-to-cell heterogeneity, stochastic signaling and is capable of handling large scale simulations (an ISD simulation takes 95.9 s and a viral infection simulation takes 2410 s on an Intel i7-1065G7 CPU). In this example of the cGAS pathway, the ABM suggests that cells may have evolved to incorporate specific degrees of cellular heterogeneity and stochasticity to reduce the number of IFNβ producing cells while maintaining cell survival. Other works have shown that these behaviors can also beneficially lead to a small subset of early IFNβ producing cells that drive the timely population level (Shalek *et al.*, 2014) and bimodal responses across the cell population (Aguilera *et al.*, 2017). In all, these simulations corroborate experimental observations and provide new insight into how cell heterogeneity and stochasticity play a role in optimizing cGAS-mediated IFNβ signaling.

Acknowledgements

The authors thank the University of Pittsburgh for providing funding and facilities.

Funding

This research was funded, in part, by the National Science Foundation, Award #1943777 and by the University of Pittsburgh.

Author Contributions

R.G. and F.S. performed computational simulations. R.G., F.S. and J.S. wrote the manuscript. R.G. and J.S. analyzed results. All authors read and edited the manuscript.

Conflict of Interest: The authors declare no conflict of interests.

References

Aguilera,L.U. *et al.* (2017) A new efficient approach to fit stochastic models on the basis of high-throughput experimental data using a model of IRF7 gene expression as case study. *BMC Syst. Biol.*, **11**, 26.

Bar-Even,A. *et al.* (2006) Noise in protein expression scales with natural protein abundance. *Nat. Genet.*, **38**, 636–643.

Brock,A. *et al.* (2009) Non-genetic heterogeneity a mutation-independent driving force for the somatic evolution of tumours. *Nat. Rev. Genet.*, **10**, 336–342.

Cohen,L.S. *et al.* (1967) Correlation between cell enlargement and nucleic acid and protein content of HeLa cells in unbalanced growth produced by inhibitors of DNA synthesis. *J. Cell. Physiol.*, **69**, 331–339.

Collins,A.C. *et al.* (2015) Cyclic GMP-AMP synthase is an innate immune DNA sensor for *Mycobacterium tuberculosis*. *Cell Host Microbe*, **17**, 820–828.

Coppey,M. *et al.* (2007) Time and length scales of autocrine signals in three dimensions. *Biophys. J.*, **93**, 1917–1922.

Cox,J.S. *et al.* (2017) The type I IFN response to infection with the type I IFN response to infection with *Mycobacterium tuberculosis* requires ESX-1-mediated secretion and contributes to pathogenesis. *J. Immunol. Ref. J. Immunol.*, **178**, 3143–3152.

Drayman,N. *et al.* (2019) HSV-1 single-cell analysis reveals the activation of anti-viral and developmental programs in distinct sub-populations. *Elife*, **8**, e46339.

Elowitz,M.B. (2002) Stochastic gene expression in a single cell. *Science*, **297**, 1183–1186.

Gao,D. *et al.* (2013) Cyclic GMP-AMP synthase is an innate immune sensor of HIV and other retroviruses. *Science*, **341**, 903–906.

Goldman,S.L. *et al.* (2019) The impact of heterogeneity on single-cell sequencing. *Front. Genet.*, **10**, 8.

Gray,E.E. *et al.* (2015) Cutting edge: cGAS is required for lethal autoimmune disease in the Trex1-deficient mouse model of Aicardi–Goutières syndrome. *J. Immunol.*, **195**, 1939–1943.

Gregg,R.W. *et al.* (2018) Mathematical modeling of the cGAS pathway reveals robustness of DNA sensing to TREX1 feedback. *J. Theor. Biol*, **462**, 148–157.

Guo,X. *et al.* (2017) Cyclic GMP-AMP ameliorates diet-induced metabolic dysregulation and regulates proinflammatory responses distinctly from STING activation. *Sci. Rep.*, **7**, 6355.

Heldt,F.S. *et al.* (2015) Single-cell analysis and stochastic modelling unveil large cell-to-cell variability in influenza A virus infection. *Nat. Commun.*, **6**, 1–12.

Hindmarsh,A.C. *et al.* (2005) SUNDIALS: suite of nonlinear and differential/algebraic equation solvers. *ACM Trans. Math. Softw.*, **31**, 363–396.

Hwang,S.-Y. *et al.* (2013) Biphasic RLR–IFN-β response controls the balance between antiviral immunity and cell damage. *J. Immunol.*, **190**, 1192–1200.

Id,T.W. *et al.* (2020) A computational model tracks whole-lung *Mycobacterium tuberculosis* infection and predicts factors that inhibit dissemination indicated in the text. *PLoS computational biology*, **16**, e1007280.

Ivashkiv,L.B. *et al.* (2014) Regulation of type I interferon responses. *Nat. Rev. Immunol.*, **14**, 36–49.

Jønsson,K.L. *et al.* (2017) IFI16 is required for DNA sensing in human macrophages by promoting production and function of cGAMP. *Nat. Commun.*, **8**, 14391.

Kim,E. *et al.* (2018) Cell signaling heterogeneity is modulated by both cell-intrinsic and -extrinsic mechanisms: an integrated approach to understanding targeted therapy. *PLoS Biol.*, **16**, e2002930.

Kreuz,L.E. *et al.* (1965) Physical properties of chick interferon. *J. Bacteriol.*, **89**, 462–469.

Lama,L. *et al.* (2019) Development of human cGAS-specific small-molecule inhibitors for repression of dsDNA-triggered interferon expression. *Nat. Commun.*, **10**,

Leviyang,S. *et al.* (2018) Investigating functional roles for positive feedback and cellular heterogeneity in the type I interferon response to viral infection. *Viruses*, **10**, 517.

Li,A. *et al.* (2019) Activating cGAS-STING pathway for the optimal effect of cancer immunotherapy. *J. Hematol. Oncol.*, **12**, 1–12.

Maekawa,H. *et al.* (2019) Mitochondrial damage causes inflammation via cGAS-STING signaling in acute kidney injury. *Cell Rep.*, **29**, 1261–1273.e6.

Milo,R. *et al.* (2015) *Cell Biology by the Numbers* 1st edn. Garland Science. New York, NY, USA.
Ng,K.W. *et al.* (2018) cGAS-STING and cancer: dichotomous roles in tumor immunity and development. *Trends Immunol.*, **39**, 44–54.
Patil,S. *et al.* (2015) Single-cell analysis shows that paracrine signaling by first responder cells shapes the interferon-b response to viral infection. *Science signaling*, **8**, ra16.
Perkel,J.M. (2019) Julia: come for the syntax, stay for the speed. *Nature*, **572**, 141–142.
Posselt,G. *et al.* (2011) Suppressor of cytokine signaling 2 is a feedback inhibitor of TLR-induced activation in human monocyte-derived dendritic cells. *J. Immunol.*, **187**, 2875–2884.
Prinz,M. *et al.* (2012) Type I interferons as ambiguous modulators of chronic inflammation in the central nervous system. *Front. Immunol.*, **3**, 67.
Qing,J. *et al.* (2004) Transforming growth factor beta/Smad3 signaling regulates IRF-7 function and transcriptional activation of the beta interferon promoter. *Mol. Cell. Biol.*, **24**, 1411–1425.
Rackauckas,C. *et al.* (2017) DifferentialEquations.jl – A performant and feature-rich ecosystem for solving differential equations in Julia. *J. Open Res. Softw.*, **5**, 15.
Raj,A. *et al.* (2008) Nature, Nurture, or Chance: Stochastic Gene Expression and Its Consequences. *Cell*, **135**, 216–226.
Rand,U. *et al.* (2012) Multi-layered stochasticity and paracrine signal propagation shape the type-I interferon response. *Mol. Syst. Biol.*, **8**, 584.
Rikard,S.M. *et al.* (2019) Multiscale coupling of an agent-based model of tissue fibrosis and a logic-based model of intracellular signaling. *Front. Physiol.*, **10**, 1481.
Roy,M. *et al.* (2019) Metabolic reprogramming dynamics in tumor spheroids: insights from a multicellular, multiscale model. *PLOS Comput. Biol.*, **15**, e1007053.
Saad,Y. *et al.* (1986) GMRES: a generalized minimal residual algorithm for solving nonsymmetric linear systems. *SIAM J. Sci. Stat. Comput.*, **7**, 856–869.
Satija,R. *et al.* (2014) Heterogeneity in immune responses: from populations to single cells. *Trends Immunol.*, **35**, 219–229.
Schulte,M.B. *et al.* (2014) Single-cell analysis uncovers extensive biological noise in poliovirus replication. *J. Virol.*, **88**, 6205–6212.
Shalek,A.K. *et al.* (2014) Single-cell RNA-seq reveals dynamic paracrine control of cellular variation. *Nature*, **510**, 363–369.
Su,C. *et al.* (2017) Herpes simplex virus 1 abrogates the cGAS/STING-mediated cytosolic DNA-sensing pathway via its virion host shutoff protein, UL41. *J. Virol.*, **91**, e02414-16.
Su,T. *et al.* (2019) STING activation in cancer immunotherapy. *Theranostics*, **9**, 7759–7771.
Sun,L. *et al.* (2013) Cyclic GMP-AMP synthase is a cytosolic DNA sensor that activates the type I interferon pathway. *Science*, **339**, 786–791.
Swain,P.S. *et al.* (2002) Intrinsic and extrinsic contributions to stochasticity in gene expression. *Proc. Natl. Acad. Sci. USA*, **99**, 12795–12800.
Wang,J. *et al.* (2016) Natural STING agonist as an "Ideal" adjuvant for cutaneous vaccination. *J. Invest. Dermatol.*, **136**, 2183–2191.
Wang,Q. *et al.* (2017) The E3 ubiquitin ligase RNF185 facilitates the cGAS-mediated innate immune response. *PLOS Pathog.*, **13**, e1006264.
Warsinske,H.C. *et al.* (2016) Computational modeling predicts simultaneous targeting of fibroblasts and epithelial cells is necessary for treatment of pulmonary fibrosis. *Front. Pharmacol.*, **7**, 183.
Wimmers,F. *et al.* (2018) Single-cell analysis reveals that stochasticity and paracrine signaling control interferon-alpha production by plasmacytoid dendritic cells. *Nat. Commun.*, **9**, 3317.
Zhao,M. *et al.* (2012) Stochastic expression of the interferon-β gene. *PLoS Biol.*, **10**, e1001249.